Molecular Therapy
Nucleic Acids
Original Article

Altered CELF4 splicing factor enhances pancreatic neuroendocrine tumors aggressiveness influencing mTOR and everolimus response

Emilia Alors-Pérez,[1,2,3,4,10] Sergio Pedraza-Arevalo,[1,2,3,4,10,11,12] Ricardo Blázquez-Encinas,[1,2,3,4] Víctor García-Vioque,[1,2,3,4] Antonio Agraz-Doblas,[1,2,3,4] Elena M. Yubero-Serrano,[1,3,5] Marina E. Sánchez-Frías,[1,6] Raquel Serrano-Blanch,[1,7] María Ángeles Gálvez-Moreno,[1,8] Francisco Gracia-Navarro,[1,2,3,4] Manuel D. Gahete,[1,2,3,4] Álvaro Arjona-Sánchez,[1,4,9] Raúl M. Luque,[1,2,3,4] Alejandro Ibáñez-Costa,[1,2,3,4,11,12] and Justo P. Castaño[1,2,3,4,11,12]

[1]Maimonides Biomedical Research Institute of Córdoba (IMIBIC), Córdoba, Spain; [2]Department of Cell Biology, Physiology, and Immunology, University of Córdoba, Córdoba, Spain; [3]CIBER Fisiopatología de la Obesidad y Nutrición (CIBERobn), Córdoba, Spain; [4]Reina Sofia University Hospital, Córdoba, Spain; [5]Unidad de Gestión Clinica Medicina Interna, Lipids and Atherosclerosis Unit, Department of Internal Medicine, Reina Sofia University Hospital, Córdoba, Spain; [6]Pathology Service, Reina Sofia University Hospital, Córdoba, Spain; [7]Medical Oncology Service, Reina Sofia University Hospital, Córdoba, Spain; [8]Endocrinology and Nutrition Service, Reina Sofia University Hospital, Córdoba, Spain; [9]Surgery Service, Reina Sofia University Hospital, Córdoba, Spain

Pancreatic neuroendocrine tumors (PanNETs) comprise a heterogeneous group of tumors with growing incidence. Recent molecular analyses provided a precise picture of their genomic and epigenomic landscape. Splicing dysregulation is increasingly regarded as a novel cancer hallmark influencing key tumor features. We have previously demonstrated that splicing machinery is markedly dysregulated in PanNETs. Here, we aimed to elucidate the molecular and functional implications of *CUGBP ELAV-like family member 4* (*CELF4*), one of the most altered splicing factors in PanNETs. *CELF4* expression was determined in 20 PanNETs, comparing tumor and non-tumoral adjacent tissue. An RNA sequencing (RNA-seq) dataset was analyzed to explore CELF4-linked interrelations among clinical features, gene expression, and splicing events. Two PanNET cell lines were employed to assess *CELF4* function *in vitro* and *in vivo*. PanNETs display markedly upregulated *CELF4* expression, which is closely associated with malignancy features, altered expression of key tumor players, and distinct splicing event profiles. Modulation of *CELF4* influenced proliferation *in vitro* and reduced *in vivo* xenograft tumor growth. Interestingly, functional assays and RNA-seq analysis revealed that *CELF4* silencing altered mTOR signaling pathway, enhancing the effect of everolimus. We demonstrate that *CELF4* is dysregulated in PanNETs, where it influences tumor development and aggressiveness, likely by modulating the mTOR pathway, suggesting its potential as therapeutic target.

INTRODUCTION

Neuroendocrine tumors (NETs) comprise a diverse and heterogeneous group of neoplasms arising from neuroendocrine cells throughout the body, with gastroenteropancreatic NETs (GEP-NETs) being their most prominent subtype. Pancreatic NETs (PanNETs) represent 62% of all diagnosed GEP-NETs,[1] with an increasing incidence over the past few years reaching 1.00 new cases per 100,000 person/year (adjusted by age),[2] and have a 90% of 5-year relative survival rate.[3] PanNETs are often detected in an advanced stage, as the lack of precise markers and specific clinical symptoms complicate early diagnosis, leading to diagnostic times between 5 and 7 years, which hinders the prompt application of effective and specific therapies.[4]

Despite their intrinsic heterogeneity,[1] PanNETs share some distinctive characteristics, such as high expression of somatostatin receptors (particularly SST_2 and SST_5), high vascularization, and alteration in different signaling pathways (as mTOR or PI3K/AKT). In fact, these features represent the main targets for medical treatment when the primary (the only curative) approach, surgery, cannot be applied or is not effective. Even though the treatments directed to SSTs (e.g., SST analogs), mTOR pathway (e.g., everolimus), or angiogenesis (e.g., sunitinib) can effectively decrease hormone hypersecretion and reduce tumor size or vascularization, in a high number of cases, tumors reduce or lose their response, often leading to greater aggressiveness, hypervascularization, or even an increase in tumor

Received 9 February 2023; accepted 1 December 2023;
https://doi.org/10.1016/j.omtn.2023.102090.

[10]These authors contributed equally

[11]These authors contributed equally

[12]Senior author

Correspondence: Sergio Pedraza-Arevalo, Maimonides Biomedical Research Institute of Córdoba (IMIBIC), Córdoba, Spain.
E-mail: b92pears@uco.es
Correspondence: Alejandro Ibáñez-Costa, Maimonides Biomedical Research Institute of Córdoba (IMIBIC), Córdoba, Spain.
E-mail: b12ibcoa@uco.es
Correspondence: Justo P. Castaño, Maimonides Biomedical Research Institute of Córdoba (IMIBIC), Córdoba, Spain.
E-mail: justo@uco.es

metastasis.[5–7] This underscores the necessity of further exploring the molecular basis of PanNETs in order to find new biomarkers and therapeutic avenues.[5] In this sense, the dysregulation of alternative splicing is increasingly regarded as a novel cancer hallmark influencing all key tumor features,[8] where an inappropriate functioning of the splicing machinery (spliceosome and splicing factors) generates aberrant splicing variants that can play oncogenic roles. In fact, dysregulation of alternative splicing is being increasingly regarded as a new epigenetic cancer hallmark associated with multiple dysfunctions in tumor cells.[9,10] Earlier evidence from our group uncovered the overexpression of aberrant splicing variants in PanNETs, SST receptor 5 (SST_5TMD4) and ghrelin (In1-ghrelin), that alter signaling pathways and basic cellular processes, thereby enhancing tumor aggressiveness,[11,12] similar to that found in various cancers.[13–19] In this context, we have previously demonstrated the status of the splicing machinery and its potential role in tumorigenesis in these tumors. Initial results revealed a broad alteration of the splicing machinery and disclosed a plausible role of *NOVA1* in PanNETs.[20]

In this scenario, in the course of pilot studies, the splicing factor CELF4 (CUGBP ELAV-like family member 4) stood out due to its notable dysregulation. CELF4 is one of the 6 members of the CELF family of RNA-binding proteins associated with regulation of pre-RNA alternative splicing.[21] Earlier studies on *CELF4* expression were conflicting, suggesting either a broad tissue expression or more restricted to nervous tissue,[22] while reports on gene mutations and variants in humans and experimental studies on rodents associated this gene to neurological, neurodevelopmental, and behavioral defects.[23–26] To date, only a limited number of studies have linked *CELF4* to cancer (colorectal and endometrial cancer and glioma),[22,27–29] but no reports have studied *CELF4* in NETs. Accordingly, this study aimed to evaluate the dysregulation and functional role of the splicing factor *CELF4* in PanNETs as well as to assess its potential role as a novel diagnostic marker and treatment target in this pathology.

RESULTS

CELF4 is dysregulated in PanNETs and is associated with clinical parameters

CELF4 expression levels were measured in a cohort of 20 primary tumors from patients with PanNETs,[20] comparing tumor with non-tumoral adjacent tissue, used as reference. This showed that *CELF4* was drastically upregulated in tumor tissues compared to their non-tumor adjacent matching ones (Figure 1A). Specificity and sensitivity comparisons using receiver operating characteristic (ROC) curve analysis of risk score showed a high predictive accuracy of the classifying *CELF4* diagnostic, with an area under the curve of 0.892 ($p = 0.001$) (Figure 1B). Higher levels of CELF4 in tumoral than non-tumoral adjacent tissue were also observed at the protein level by immunohistochemistry (IHC), including not only exocrine tissue but also islets of Langerhans, which would be the neuroendocrine non-tumoral tissue of reference (Figure 1C). Analysis of clinical parameters revealed that *CELF4* expression was associated with lower abdominal pain and lower metastasis, two relevant malignancy features in PanNETs (Figures 1D and 1E).

CELF4 modulation suggests its role in aggressiveness of PanNETs

Having found associations between *CELF4* expression levels and relevant clinical data linked to tumoral features, we next aimed to explore the role of *CELF4* in PanNET aggressiveness and its potential as therapeutic target. To this end, two widely PanNET cell models (QGP-1 and BON-1) were employed. First, *CELF4* expression levels were assessed in the two cell lines (Figure S1A), which showed that both cell lines have appreciable mRNA levels amenable to manipulation through genetic alterations. After 72 h *CELF4* silencing by specific small interfering RNAs (siRNAs), its expression levels decreased by 40% and 20% in QGP-1 and BON-1 cells, respectively, as compared to scramble siRNA (used as control) (Figure S1B). On the other hand, *CELF4* was overexpressed in both cell lines with a specific plasmid, obtaining substantial increases of mRNA levels after 72 h (Figure S1C). Interestingly, *CELF4* silencing with the specific siRNA significantly reduced the proliferation rate in both cell lines (Figure 2). In QGP-1 cells, the effect was long lasting (48 and 72 h) and appeared quantitatively more prominent (at 24 h, cells had not grown enough after starving), whereas in BON-1 cells, a significant reduction was observable at 24 and 48 h (Figure 2A). Consistent with these results, *CELF4* overexpression resulted in the opposite effect, an increase in proliferation in both cell lines, being most prominent in BON-1 after 48 h (Figure 2B). Surprisingly, *CELF4* silencing increased QGP-1 apoptosis at 48 h but did not affect BON-1 in this regard, suggesting a complex intervention in molecular mechanisms that depends on cellular context (Figure 2C). Furthermore, the antitumoral effects exerted by *CELF4* silencing *in vitro* were closely reproduced in an *in vivo* xenograft mice model. Specifically, xenograft tumors generated by inoculated BON-1 cells followed for 2 weeks drastically slowed down their growth after an intratumoral injection with *CELF4*-silencing siRNA but not when scrambled siRNA was injected (Figure 2D); validation of *CELF4* reduction is shown in Figure S1D. In addition, as a validation of these results based on *CELF4* silencing, we tested two additional siRNAs in both cell lines, which exerted the same results for *CELF4* expression reduction and similar results in cell proliferation, suggesting that such an effect is not caused by off-target genes (Figures S1E and S1F). On the other hand, no appreciable changes were observed in tumor growth when *CELF4* was overexpressed in BON-1 xenografted tumors (data not shown).

Cancer therapy's effectiveness can be triggered by modulation of *CELF4*

We next asked whether *CELF4* expression levels could influence the response of PanNET cells to the currently available pharmacological treatment for these tumors: mTOR inhibitors (e.g., everolimus), SST analogs (e.g., lanreotide), and antiangiogenic drugs (e.g., sunitinib). To answer this question, we tested the *in vitro* effects of everolimus, lanreotide, and sunitinib in QGP-1 and BON-1 cells wherein *CELF4* was either overexpressed or silenced (Figures 3A–3C). Results from this experimental approach revealed a markedly distinct responsiveness of both cell lines to the three drugs and an intriguingly differential interaction of *CELF4* with each of the drugs. Specifically, in both cell types, silencing of *CELF4* expression seemed to enhance

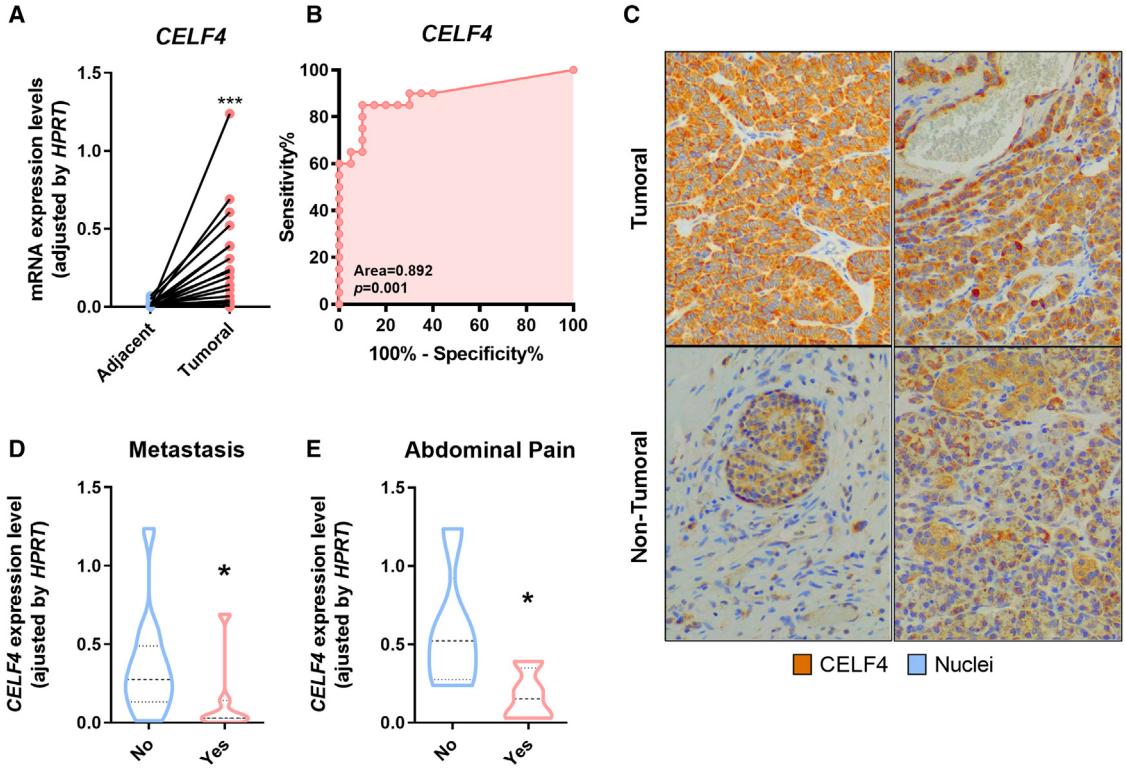

Figure 1. *CELF4* dysregulation in PanNETs

(A) *CELF4* expression levels in FFPE cohort of 20 patients with PanNETs; tumor tissue is compared with controls (non-tumor adjacent tissue). Data are represented by relative mRNA levels normalized by *HPRT* expression levels. (B) *CELF4* ROC curve in FFPE cohort of PanNET tissue compared with non-tumor adjacent tissue (used as control). Data are represented by relative mRNA levels normalized by *HPRT* expression levels. (C) Representative IHC 20× images of CELF4 IHC analysis in PanNET FFPE samples vs. non-tumoral adjacent tissue. Orange color represents CELF4 staining, and blue color represents hematoxylin counterstaining of nuclei. (D and E) *CELF4* expression levels in tumor tissue FFPE cohort association with clinical parameters (metastasis and abdominal pain). Data are represented by relative mRNA levels normalized by *HPRT* expression levels. Values represent the median and interquartile range. Unpaired t test was performed to assess statistical analysis between groups. Asterisks indicate values that significantly differ from control (*$p < 0.05$, ***$p < 0.001$).

the antiproliferative action of everolimus, whereas, in contrast, *CELF4* overexpression did not interfere with the response to everolimus, which clearly overrode the enhanced proliferation caused by overexpression of the gene (Figure 3A). In clear contrast, cells were poorly responsive to lanreotide treatment, which reduced proliferation only in BON-1 cells (and not consistently) and, paradoxically, increased it long term (72 h) in QGP-1 cells, while these marginal effects did not seem to be influenced by *CELF4* silencing or overexpression (Figure 3B). Interestingly, QGP-1 and BON-1 cells were unresponsive to sunitinib treatment under *in vitro* basal culture conditions, whereas this kinase inhibitor significantly decreased the enhanced proliferation rate in BON-1 cells overexpressing *CELF4* (Figure 3C). Thus, the PanNET cell models tested showed a limited, barely informative response to lanreotide or sunitinib but displayed a robust responsiveness to everolimus, which appeared to be clearly influenced by *CELF4* expression levels.

Signaling pathways associated with *CELF4* genetic alteration

The functional interplay between *CELF4* expression in PanNET cells and their response to everolimus prompted us to further investigate the relationship of this splicing factor to the mTOR pathway, the primary target of everolimus. To this end, we evaluated changes in phosphorylation in QGP-1 and BON-1 cell lines after *CELF4* silencing (or scramble transfection, as a control), assaying an ample panel of proteins that provide a complete collection of the molecular components of the mTOR pathway by means of a phospho-antibody array. Results from this assay enabled the identification of a total of 17 proteins significantly phosphorylated differently after *CELF4* silencing (showed in Tables S1 and S2). Of those, 8 proteins (47%) were altered in QGP-1 cells, while 14 (82%) were selectively altered in BON-1 (Figures 4A and 4B). This fact indicates a clear dysregulation of this pathway in relation to *CELF4* expression. Among these changes, important mTOR regulators can be found altered in both cell lines, like AKT or TSC2, a key activator and inhibitor of the pathway, respectively. Moreover, BAD, related to apoptosis regulation, was also similarly altered after *CELF4* silencing in both cells, although the specific phosphosites affected were different, being apparently more tightly regulated in BON-1.

In addition, to further delineate and understand these findings, we designed a signaling network model with altered phosphoproteins,

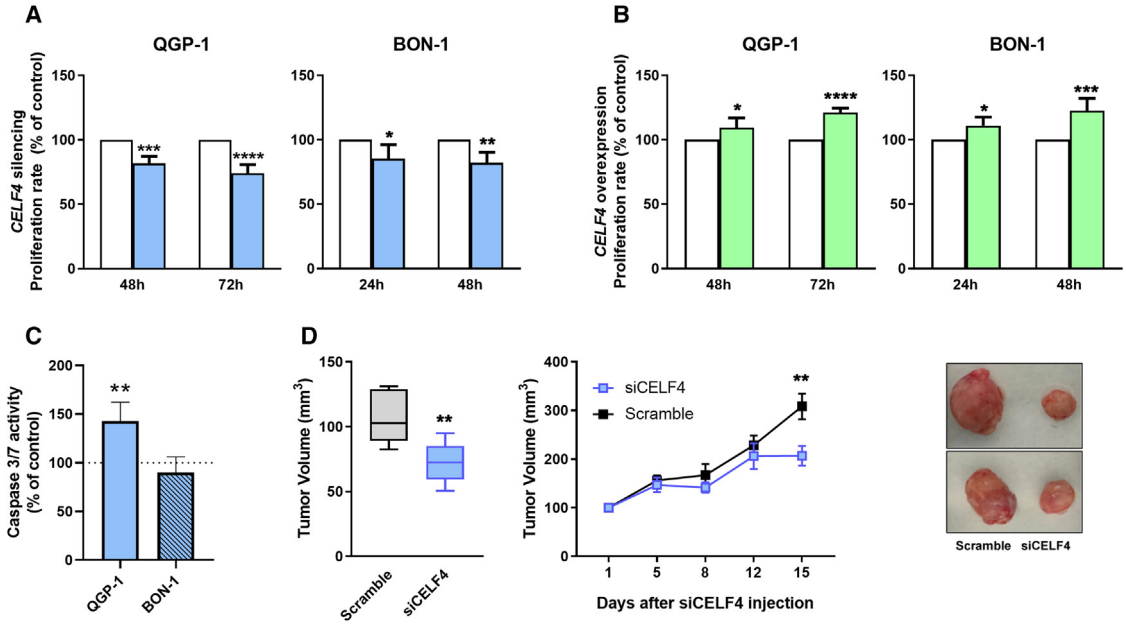

Figure 2. Functional effects of *CELF4* modulation in QGP-1 and BON-1 cell lines

(A and B) Changes in cell proliferation at 24, 48, and/or 72 h of QGP-1 and BON-1 cell lines in response to (A) *CELF4* silencing or (B) *CELF4* overexpression. Control (scramble or mock plasmid, respectively) was set at 100%. Four independent experiments were included. (C) Apoptosis assay in both cell lines at 48 h after silencing *CELF4*. Four independent experiments were included. (D) Left: relative tumor volume of BON-1 xenografted mice in *CELF4* siRNA-injected mice compared with scramble-injected mice at time of euthanasia (15 days after silencing); tumor volume is expressed as mm^3. Middle: volume growth in BON-1 xenografted mice after *CELF4* siRNA injection; tumor volume is expressed as mm^3 and was measured in all the mice every 3–4 days using a caliper. Right: representative picture of paired xenografted tumors with *CELF4* downregulation (right) compared with scramble (left). Five mice were included in the study. Values represent the mean ± SD or median and interquartile range. Unpaired t test was performed to assess statistical analysis between groups. Asterisks indicate values that significantly differ from control (*$p < 0.05$, **$p < 0.01$, ***$p < 0.001$, ****$p < 0.0001$).

which enables the prediction of interactions and the detection of possible intermediates altered in the pathway. Despite the differences observed in the phospho-assay, both cell lines shared some insights in the subsequent functional network. In QGP-1 cells, the model yielded 26 nodes and 46 edges (Figure 4C), whereas in BON-1 cells, the signaling network model comprised 24 nodes and 42 edges (Figure 4D). In both models, an expected alteration of downstream phosphorylation of mTOR canonical pathway was observed, with CDK5 and ERN1 mostly altered, followed by MAP3K5. Finally, the main phosphorylation changes (AKT and TSC2) were validated by western blot in both cell lines (Figures 4E and 4F) to confirm the results. Taken together, these results support the contention that changes in the expression of a relevant splicing factor, *CELF4*, substantially and similarly influences key elements in a signaling cascade that is both a core route and therapeutic target in PanNETs.

Transcriptomic alterations associated with *CELF4* expression levels

To explore the putative significance of *CELF4* alteration in PanNETs, we first analyzed a previously published RNA sequencing (RNA-seq) dataset corresponding to 11 patients with PanNETs (mean age of patients: 52.7 years old; 54% males; 90.9% low-grade tumors; GEO: GSE118014), who were divided into two groups based on *CELF4* expression levels: high (n = 5) and low levels (n = 6), selected under quartile 1 and over quartile 3 of *CELF4* expression, respectively. Unsupervised analysis revealed that low- and high-*CELF4*-expressing tumors were clearly segregated according to gene expression (Figure S2A). A total of 357 genes (1.15%) were differentially expressed according to the expression of *CELF4*, suggesting that *CELF4* may act as a global transcriptional regulator in PanNETs. From these, 46.78% were upregulated and 53.22% downregulated (Figure S2B; Table S3). Specifically, we observed an inverse correlation with the tumor suppressors *TP53* and *CDKN2B* and a direct correlation with *TSC1* and *BAD* (Figure S2C). To get further insights into the biological functions affected by differentially expressed genes, we used DAVID software and gene set enrichment analysis (GSEA) to perform KEGG analysis. Among the top significant KEGG-enriched hits in the low-expression group of *CELF4*, relevant relationships were found with interleukin-6 (IL-6), ERK1 and ERK2, JNK, or MAPK activity (underlined) (Figure S2D). In contrast, high *CELF4* expression was closely associated with TORC1 signaling and regulation of mRNA, aside from neural-related pathways (Figures S2E and S3).

To study gene expression changes driven by *CELF4* alteration, we silenced its expression in QGP-1 and BON-1 cell lines and then performed RNA-seq. In QGP-1 cells, we found 1,214 upregulated genes and 505 downregulated genes after *CELF4* silencing. In contrast, in

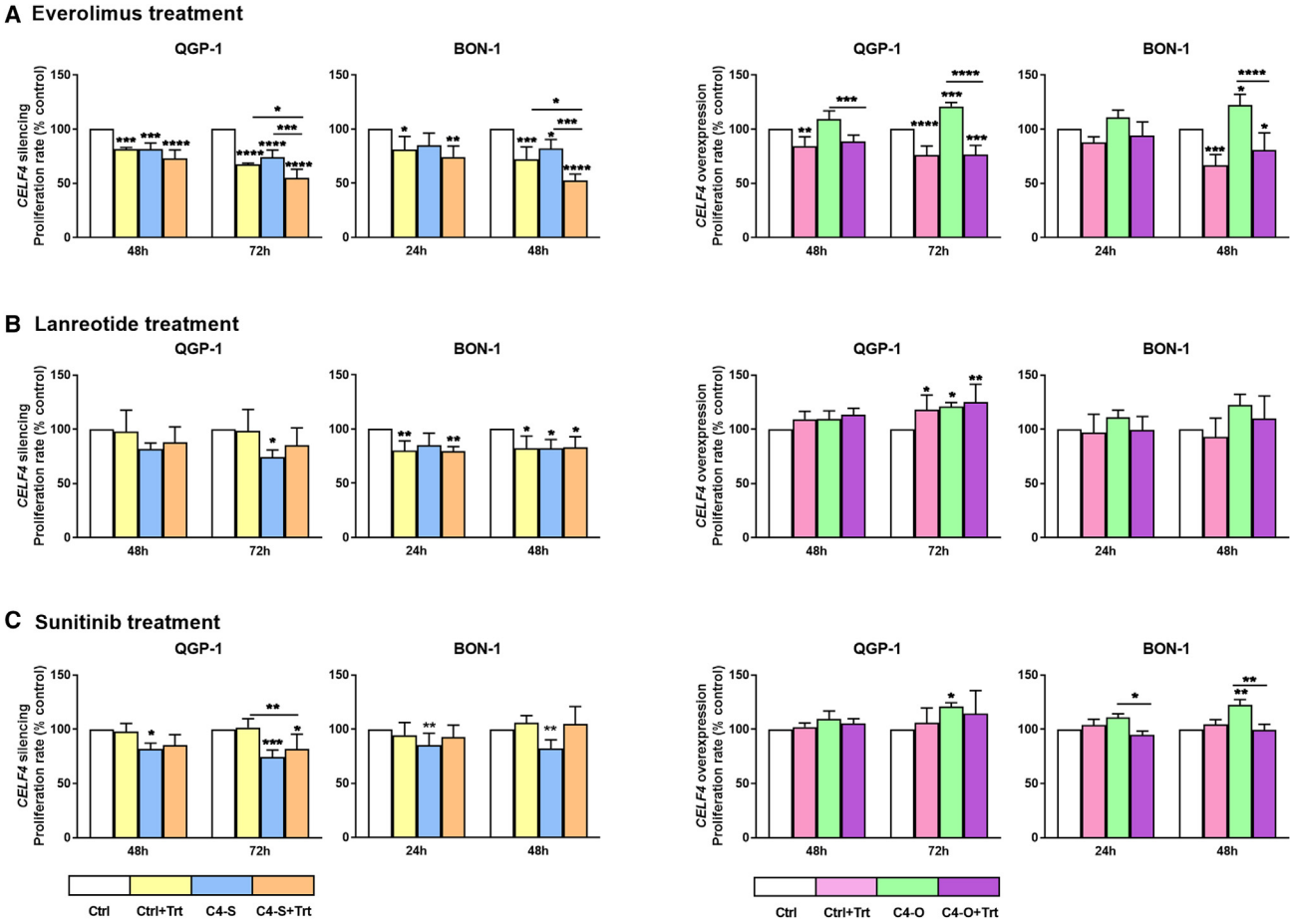

Figure 3. *CELF4* modulation alters the effect of classical PanNETs treatments in cell models

Changes in proliferation rate of BON-1 and QGP-1 cell lines, at 24, 48, and/or 72 h, in response to *CELF4* silencing (left) or overexpression (right) and after treatment with (A) everolimus, (B) lanreotide, or (C) sunitinib. Control (untreated scramble- or mock-plasmid-transfected cells, respectively) was set at 100%. Four independent experiments were included. One-way ANOVA test was performed to assess statistical differences between groups. Values represent the mean ± SD. Asterisks indicate values that significantly differ from control (*$p < 0.05$, **$p < 0.01$, ***$p < 0.001$, ****$p < 0.0001$).

BON-1, we found 1121 genes upregulated and 1,337 downregulated (Figure 5A; Tables S4 and S5). Hallmark enrichment analysis unveiled that differentially expressed genes belong to important cancer-related processes, and specifically, we found cell-cycle-related genes (G2M checkpoint and E2F targets) that were commonly downregulated after *CELF4* silencing in both cell lines (Figure 5B). However, the rest of the pathways altered were heterogeneous between both cell lines.

A specific examination of mTOR-related genes revealed common alterations in gene expression in both QGP-1 and BON-1 cell lines. Some genes directly taking part in the main mTOR signaling pathway were altered, including an overexpression of mTOR activator *AKT1S1* and downregulation of several effectors/targets, like *BCAT1*, *CDC25A*, and *SKP2*. Additionally, components of cell metabolic routes strongly linked to mTOR were also downregulated, including *MTHFD2*, *RRM2*, *SLC1A4*, and *SLC37A4*. Interestingly, QGP-1 and BON-1 showed different alterations in the expression of the apoptotic markers *FOXO1A* and *BBC3* (Figure 5C).

Splicing dysregulation associated with *CELF4* expression levels

Further exploratory analysis of the human PanNET RNA-seq dataset revealed that 62 changes in spliceosomic events were associated with *CELF4* expression (Figure S4A; Table S6). These splicing pattern differences were mainly attributable to exon skipping, alternative 5′ splice sites, and alternative first exon splicing events, which were the most altered as compared to normal-overall event pattern (considering *CELF4* expression) (Figure S4B).

To gain additional insight into and experimental support for the role of *CELF4* in PanNETs, we performed an RNA-seq analysis after silencing *CELF4* in QGP-1 and BON-1 cell lines. This approach revealed 291 and 358 differentially spliced events in QGP-1 and BON-1 cell lines, respectively (Figure 6A; Tables S7 and S8).

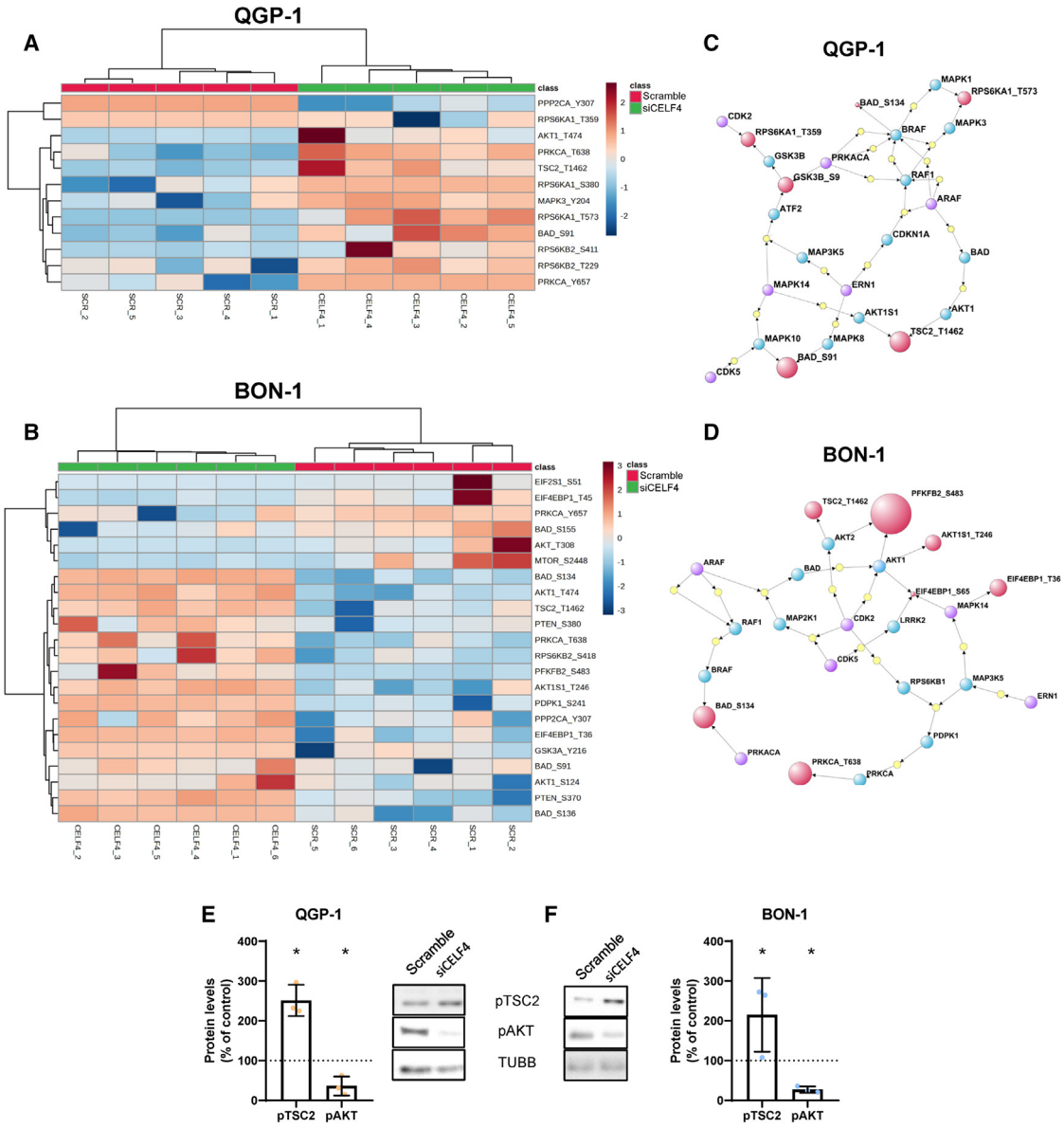

Figure 4. Influence of *CELF4* expression on the functional profile of phosphoprotein of the mTOR pathway

(A and B) Unsupervised clustering analysis of phosphorylated protein levels of mTOR pathway components in *CELF4*-silenced QGP-1 (A) and BON-1 (B) cells (1; green) compared to scramble control (0; red). (C and D) PHONEMeS solution model of signaling for mTOR phospho-antibody array after *CELF4* silencing in QGP-1 (C) and BON-1 (D). Target proteins (purple circles) correspond to the highly regulated proteins, which were connected to its target phosphorylation sites (red circles) through intermediary kinases (blue circles). Central kinases, which were also identified by kinase activation prediction, are shown as intermediary kinases with small yellow circles. (E and F) Validation by Western blot assay of TSC2 and AKT phosphorylation in QGP-1 (E) and BON-1 (F) with representative images, normalized by TUBB.

Alternative splicing patterns affected were mainly exon skipping and alternative first exon (Figure 6B). Only slight differences were found in the length on skipped/alternative spliced exons and flanking introns (Figures S5A and S5B), suggesting that this parameter is not relevant for CELF4 action. In addition, frameshifting changes derived from alternatively spliced exons were similar between included and excluded events in both cell lines (Figure S5C). Parallelly, specific alternative splicing events were explored, showing increased inclusion of exons leading to isoform switching of *BCL2*, *CCDC50*, and *PTPMT1*, involved, respectively, in apoptosis, cell-cycle regulation, and mTOR signaling (Figure 6C).

DISCUSSION

Splicing dysregulation is increasingly considered a novel cancer hallmark influencing all key tumor features.[8] In PanNETs, our earlier work unveiled the overexpression of aberrant splicing variants

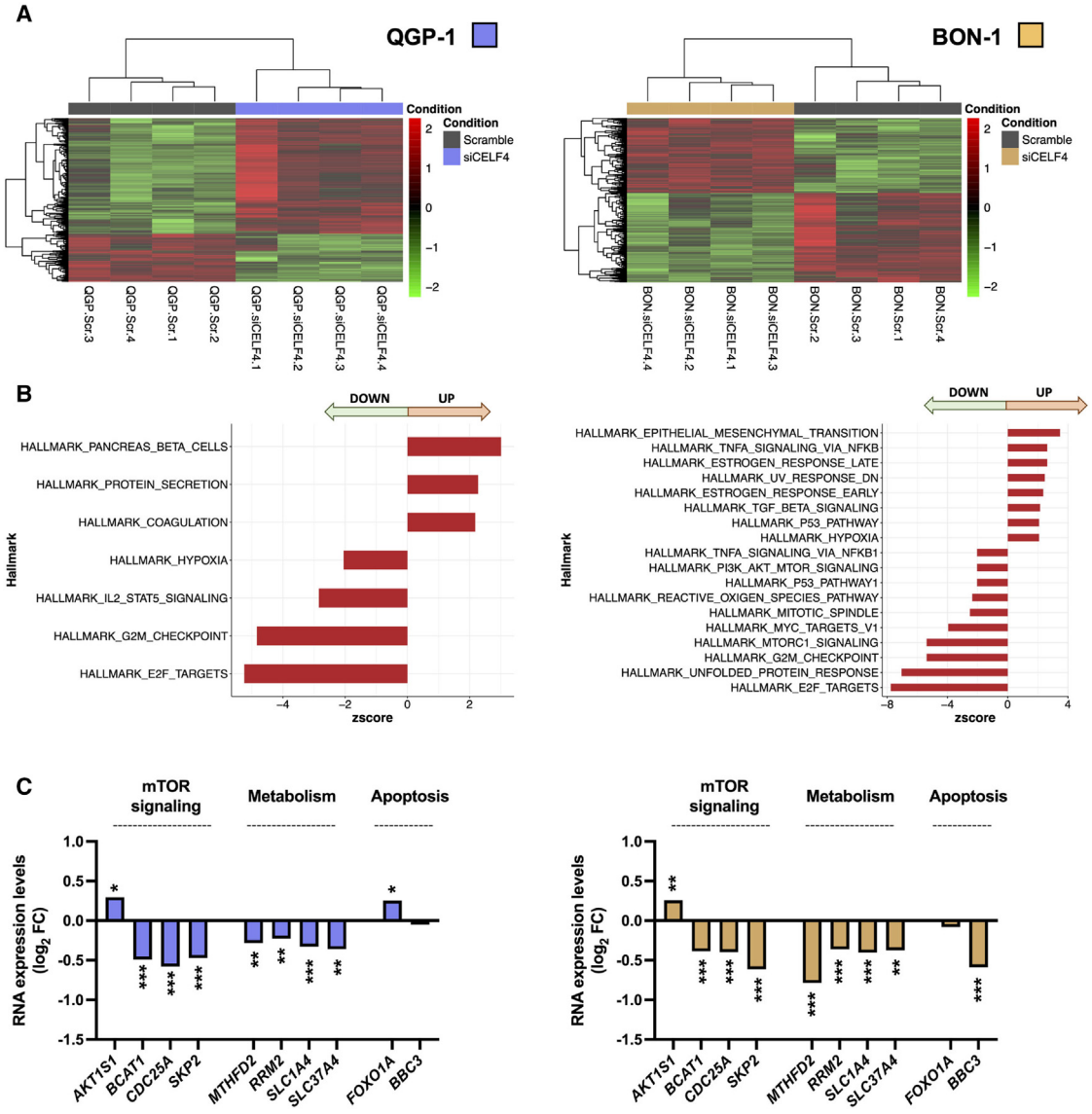

Figure 5. Molecular signature associated with *CELF4* silencing from RNA-seq analysis

(A) Hierarchical heatmaps generated with the expression levels of the top genes that contribute most to the discrimination between scramble (gray) and *CELF4*-silenced (colored) QGP-1 (left) and BON-1 (right) cell lines. (B) GSEA Hallmark pathway analysis with altered genes after *CELF4* silencing in QGP-1 (left) and BON-1 (right) cells. A positive *Z* score value indicates enrichment in *CELF4*-silenced cells, while a negative value indicates an enrichment in scramble-transfected cells. (C) RNA expression of altered genes from mTOR signaling, cellular metabolism, and apoptosis pathways after *CELF4* silencing in QGP-1 (left) and BON-1 (right) cell lines. Values are expressed as $\log_2$ of the fold change (FC). Four different experiments were performed for each cell line. Asterisks indicate significant differences (*$p < 0.05$, **$p < 0.01$, ***$p < 0.001$) from DESeq2 Wald test.

that impart oncogenic properties,[11,12] similar to that found in numerous cancers.[13–19] More recently, we discovered that the splicing machinery, which involves multiple splicing factors and may underlie tumorigenesis, is altered in PanNETs.[20] These findings are in agreement with the idea derived from biocomputational analysis of large datasets that alteration of the splicing machinery can result in dysregulated splicing in sets of functionally related genes, which may lead to an imbalance in relevant processes in tumors.[30,31] However, the status and dysregulation of the splicing machinery largely varies for each type of tumor, and therefore, the detailed role and putative oncogenic contribution of individual altered components have to be assessed in their appropriate context. In this study, we describe that the splicing factor *CELF4* is altered in PanNETs, where its dysregulation may enhance tumor aggressiveness by acting through the mTOR pathway, which may, in turn, influence PanNET cell response to everolimus.

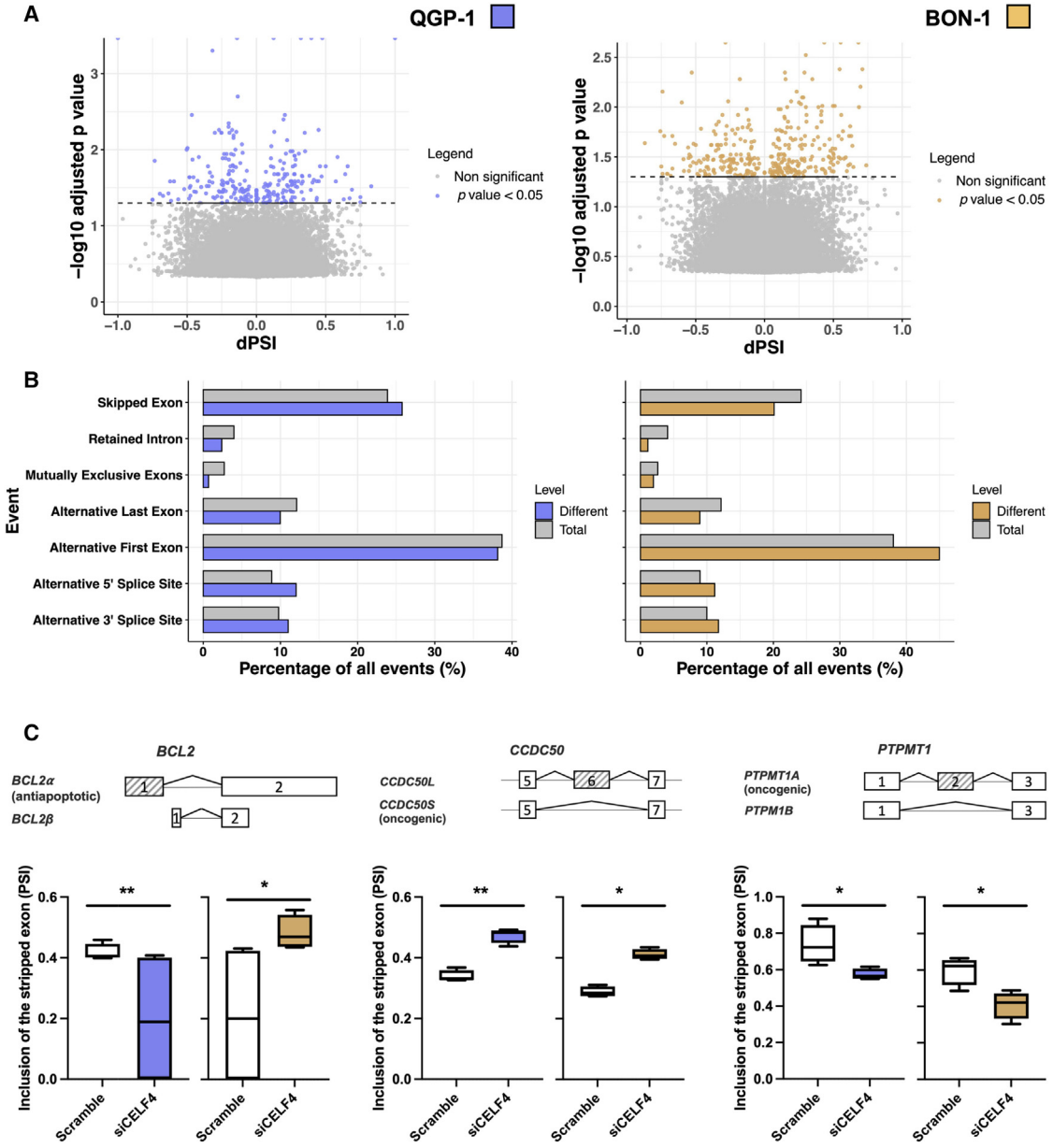

Figure 6. *CELF4* silencing modifies alternative splicing profile in PanNET cells

(A) Volcano plot showing delta percent spliced in (dPSI) of significantly altered splicing events (colored dots) in QGP-1 (left) and BON-1 (right) cell lines after silencing *CELF4* compared to scramble control. Significance was calculated by Fisher's exact test. (B) Alternative splicing event characterization of RNA-seq data after *CELF4* silencing. Percentage of splicing events detected (gray) and significantly different events after *CELF4* silencing (colored) are classified depending on their type, showing different frequencies in QGP-1 (left) and BON-1 (right) cell lines. (C) Alternative splicing modifications under *CELF4* silencing of key genes, *BCL2*, *CCDC50*, and *PTPMT1*, in QGP-1 (left) and BON-1 (right) cells. Four different experiments were performed for each cell line. Asterisks indicate significant differences (*$p < 0.05$, **$p < 0.01$).

Our initial discovery derived from the observation that this splicing factor is overexpressed in tumor tissue compared to non-tumoral adjacent tissue in paired samples, which was well in line with our previous study, where the vast majority of splicing machinery components studied were upregulated in PanNET tissue.[20] The use of surrounding non-tumoral tissue as a reference poses obvious limitations but is commonly accepted as a means for biomarker discovery in NETs, where the access to fully normal tissue of origin is very difficult if not practically impossible. Nevertheless, the relevance of the discovery of this altered marker is reinforced by the confirmatory immunocytochemical data and by its quantitative inverse association with the rate of metastasis and abdominal pain, which jointly support the notion that high levels of *CELF4* expression could be explored as a potential tumor biomarker in patients with less

metastasis and pain and hence where tumor initiation might be more difficult to identify. These results could seem counterintuitive since a lower chance of metastasis is obviously a good prognosis factor; however, we have shown, through the RNA-seq analysis, that *CELF4* might participate in a wide range of cellular processes and that not all of them are potentially malignant. This is the case of increased epithelial mesenchymal transition or hypoxia and decreased p53 pathway in BON-1 cells after *CELF4* silencing, while, in QGP-1, hypoxia decreases, and coagulation, which has been related to adaptive response in cancer,[32] seems to increase. All these results show a complex behavior of *CELF4* that is strongly affected by the cellular context and invite the development of a further and deeper examination.

The present findings on *CELF4* are completely original since, although the role of *CELF4* in alternative splicing and neurological pathophysiology is well established,[21,23–26] its precise implication in cancer is still poorly understood. In colorectal cancer, bioinformatic analysis of open databases suggested a prognostic role involving an intronic variant,[27] reviewed in Dasgupta and Ladd,[22] while in endometrial cancer, *CELF4* expression seems to be downregulated due to hypermethylation and may also provide prognostic information.[29] Very recently, *CELF4* has been linked to oncogenic splicing alterations in high-grade diffuse glioma, not necessarily through mutational but via transcriptional or epigenetic regulation.[33] Thus, altogether, these emerging data emphasize that the expression of *CELF4* in PanNETs and its reported epigenetic control[25] warrants additional, detailed study.

Accordingly, we next studied the functional consequences of *CELF4* expression modulation (silencing and overexpression) using two PanNET model cell lines. This revealed that high *CELF4* expression levels directly increased proliferation of BON-1 and QGP-1 cells, whereas its silencing exerted the opposite effect, decreasing cell proliferation. These results compare favorably with our recent findings in PanNETs studying a related splicing factor, *NOVA1*,[20] but also in the most aggressive pancreatic adenocarcinoma cell models, where manipulation of *SF3B1* caused these same effects.[34] These parallel observations are in line with recent findings from our group and other labs[35–37] and collectively argue in favor of the idea that not only mutations but also transcriptional (and epigenetic) alterations of specific components of the splicing machinery can entail functionally relevant consequences for key cell processes. Remarkably, *in vivo* data with xenograft mice provide proof of concept that *CELF4* silencing in PanNET BON-1 cell-derived tumors can counteract cell proliferation and blunt tumor growth, paving the way to further explore the therapeutic potential of CELF4 in these rare tumors. Nevertheless, xenograft tumors overexpressing *CELF4* did not show significant changes in growth compared to their empty vector control, probably due to the intrinsic high levels of *CELF4* expression in these cells, which may impair further activation of the effects of this gene.

To further understand the possible role of *CELF4* in PanNETs and its relation to splicing regulation, we performed a biocomputational analysis of a publicly accessible RNA-seq dataset (GEO: GSE118014). This showed that high or low *CELF4* expression levels are distinctly associated with the expression of a discrete percentage of genes (1.15%), which includes a high representation of relevant cancer-related genes. In particular, we observed an inverse correlation with two tumor suppressors: one that is widely known to hold strong links with NETs, *TP53*,[38] and a related one, *CDKN2B*, that has also been linked to PanNETs and advanced neuroendocrine neoplasms.[39,40] In contrast, *CELF4* expression levels were directly correlated with *TSC1* and *BAD*, two pivotal intermediaries of PI3K/Akt and EGFR/MAPK pathways,[6,41] whose expression appeared to be enriched in relation to *CELF4* expression in the GSE/DAVID analysis. Moreover, when the analysis of *CELF4* was focused on splicing, we observed that high/low *CELF4* expression was associated with a distinct pattern of splicing events, mostly due to a higher usage of exon skipping and alternative first exon, differences that have been shown to be linked to alterations in the resulting transcript profile and proteome diversity and function.[11,12,14,19,42] These interesting results led us to perform an RNA-seq analysis in our cell models, QGP-1 and BON-1, after *CELF4* silencing, to better understand the functional relevance and molecular meaning of its loss. This experiment showed a clear dysregulation in key pathways (mTOR, MYC, p53, etc.) and cancer hallmarks, including cell-cycle control, epithelial-mesenchymal transition, and hypoxia. In the same direction, a remarkable change in alternative splicing was observed, indicating that *CELF4* could play a highly relevant role in RNA regulation of PanNETs. In fact, there was a great increase in the oncogenic *CCDC50L* isoform[43] after *CELF4* silencing, directly linking its primary function—splicing—to aggressive features. Nevertheless, these changes do not completely parallel those described in the public dataset. However, as the results from the two cell lines also differ in some relevant molecules and pathways, this suggests that the specific cellular—and tissue—context is critical and, thus, that it is expectable that highly heterogeneous tumors, such as PanNETs, show differences from the *in vitro* models. Notwithstanding this, we consider that our present results provide convincing evidence to suggest that *CELF4* can exert a relevant function in PanNETs through regulation of the expression and splicing profiles of functionally and pathologically relevant genes, thereby inviting us to explore in more detail their potential relationships.

From a mechanistic perspective, the suggestive biocomputational evidence pointing toward a CELF4-dependent alteration in the PI3K/Akt/mTOR pathway was confirmed by functional *in vitro* assays, where modulation of *CELF4* expression in PanNET cells influenced their response to everolimus, a paradigmatic mTOR pathway inhibitor and first-line drug for the treatment of these tumors.[44] Thus, whereas *CELF4* silencing enhanced the antiproliferative effect of everolimus, its overexpression did not interfere with the inhibitory capacity of the drug. Furthermore, detailed inspection of this signaling cascade with a dedicated phosphoarray illuminated the discrete set of specific components that are particularly influenced by *CELF4* expression in each cell line. Interestingly, those precise targets mostly differed between BON-1 and QGP-1 cells, which is not surprising given the known fundamental differences of these cell models at multiple levels, from genetic to phenotypic and also functional,[45,46] which

nevertheless also reflect the remarkable multilayered heterogeneity of PanNETs.[1,47–49] Despite these differences, the main inhibitor of mTOR, TSC2, was increasingly phosphorylated in both cell lines, while one of the main activators, AKT1, was significantly inhibited, showing a general decrease of mTOR signaling. Actually, to confirm this fact, gene expression analysis from RNA-seq data after *CELF4* silencing showed that some of mTOR effectors/targets, including *BCAT1*,[50] *CDC25A*,[51] and *SKP2*,[52] were downregulated, while *AKT1S1*,[53] an inhibitor of mTOR, was upregulated.

In addition, other related pathways involved in cell metabolism are also downregulated, showing a significant decrease after *CELF4* silencing. Specifically, *MTHFD2* is involved in purine synthesis, and it has been shown to be activated by mTOR action,[54] while being shown to increase mTOR activation through purine accumulation;[55] *RRM2*, a ribonucleotide reductase, is activated by this pathway,[56] and it has been also shown that its high expression is linked to poor prognosis in pancreatic cancer, possibly due to the activation of PI3K/AKT/mTOR;[57] *SLC1A4* is an amino acid transporter, and its expression has also been linked to mTOR activation;[58] finally, *SLC27A4*, a fatty acid transporter, has been related to stearic acid transport via PI3K-mTOR regulation in other mammals.[59] On the other hand, since CELF4 acts mainly as splicing factor, we observed that these alterations in the mTOR pathway could be due, at least in part, to alternative splicing of *PTPMT1A*,[60] a phosphatase whose shorter isoform (increased under *CELF4* silencing) has been linked to a mTOR inhibition. Thus, these results reinforce the idea that the presence of high *CELF4* levels in PanNETs can influence, likely through mechanisms involving splicing and gene expression regulation, the mTOR pathway, a master signal that impacts cell survival, proliferation, growth, and metabolism, and that it can also affect angiogenesis and metastasis.[61,62] Indeed, the comprehensive molecular landscape of PanNETs revealed that a notable proportion of genes related to this pathway are mutated or altered in these tumors, including from *TSC1* and *TSC2* to *PTEN* or *PIK3CA*.[6,41,63–65]

Interestingly, as mentioned above, this analysis reinforced the notion that these two cell models are different in the sense that *CELF4* acts distinctly therein, in a cellular context. In fact, *CELF4* silencing induced different alterations in the phosphorylation of relevant proteins, such as BAD, an apoptosis-related protein that is more phosphorylated in the S91, in both cell lines, while BON-1 shows another 2 phosphorylation sites altered under *CELF4* silencing. This protein in supposed to be inactivated, and then unable to promote apoptosis, when phosphorylated, which is partially controlled by the PI3K-AKT-mTOR pathway.[66] In line with this difference, two proapoptotic genes, *FOXO1A*[67] and *BBC3*,[68] are increased and decreased by *CELF4* silencing in QGP-1 and BON-1, respectively. This observation fits nicely with apoptosis results, where we observed that QGP-1 increased its apoptotic response to *CELF4* silencing while BON-1 stayed unaltered. Although further experiments are needed to confirm and better understand the molecular causes of this effect, we have observed a differential splicing of *BCL2*[69] in these cell lines where *CELF4* silencing decreased its antiapoptotic isoform in QGP-1 but increased it in BON-1, which could play a relevant role in mediating their distinct functional response.

In summary, our results revealed that the splicing factor *CELF4* is dysregulated in human PanNETs. Inhibition of *CELF4* levels reduces multiples cancer features in PanNET cell lines, and its alteration can contribute to tumor development and a more aggressive phenotype, impacting the mTOR signaling pathway. Future studies should be aimed at further exploring the role of *CELF4* and the detailed contribution of individual mTOR pathway components altered after its silencing, which will help to elucidate the oncogenic role of these novel molecules in the PanNET field as well as to define their potential as actionable therapeutic targets.

MATERIALS AND METHODS

Patients and samples

Formalin-fixed, paraffin-embedded (FFPE) samples from 20 primary PanNETs were collected, and tumor tissue and non-tumor adjacent tissue (used as reference-control) from the same piece were separated by expert pathologists and extracted. Clinical parameters from the patients have been detailed elsewhere previously[20] and are summarized in Table S9. The mean age of PanNETs patients was 55 years old. This study was approved by the Ethics Committee of the Reina Sofia University Hospital (Cordoba, Spain) and was carried out according to the Declaration of Helsinki. Patients were treated following national and international clinical practice guidelines, and a written informed consent was signed before sample inclusion. FFPE samples were obtained from the Andalusian Biobank (S1900499).

Immunohistochemical analysis

IHC was performed to study the protein expression levels of CELF4 in FFPE PanNET samples, using standard procedures, as previously reported,[15] with a commercial antibody (ab171740, 1:100 dilution, ABCAM, Cambridge, UK).

Gene expression profiling and splicing variants analysis

We analyzed 33 transcriptomes of human non-functional PanNETs deposited in NCBI (GEO: GSE118014).[70] Raw paired-end FASTQ files were downloaded (approximately 180 million paired-end reads per sample) and were aligned to the human genome (hg19) using Tophat.[71] Differentially expressed genes (DEGs) were identified using high-throughput sequence (HTSeq) and DESeq tools.[72,73] Differential expression of RNA transcript levels was performed with R packages, and a minimum of 3 counts per gene in more than two independent samples was required. To perform a clustering for *CELF4* expression, we generated four groups in terms of Q1 (high) or Q4 (low) expression using mclust.[74] A fold change of >1.5 with a q value <0.05 were used to call DEGs. Signaling pathway enrichment was analyzed using the GSEA tool[75] and DAVID Resources.[76]

To detect splicing variants, we quantified transcripts using Salmon[77] with the v.34 release of human GENCODE transcriptome.[78] To calculate the relative abundances of splicing events, the same high- and low-expression groups of *CELF4* expression used above were applied

to detect a differential splicing ($p < 0.05$) of the percent spliced in index (PSI or Ψ) using SUPPA2 software.[79] Classification of splicing events profiling was established into 7 types of events according to their splicing pattern: skipped exon, mutually exclusive exons, alternative 5′ splice site, alternative 3′ splice site, retained intron, alternative first exon, and alternative last exon.

To explore direct transcriptomic effects of *CELF4* depletion, we performed RNA-seq (2 × 150 paired-end and 50 M reads; AZENTA Life Sciences, Leipzig, Germany) of QGP-1 and BON-1 cell lines after silencing *CELF4* (n = 4). Gene expression and alternative splicing were analyzed using the same methods explained above.

Cell lines

To explore the functional relevance of the selected molecule under study, two human cell lines were employed as PanNET models, the carcinoid-like BON-1, kindly provided by Dr. M.C. Zatelli (University of Ferrara, Ferrara, Italy), and the somatostatinoma-derived QGP-1 cell line, kindly provided by Dr. K. Öberg (University of Uppsala, Uppsala, Sweden), as previously reported.[11,12]

Specific silencer siRNA (SR311214, Origene, Rockville, MD, USA) was employed to decrease *CELF4* expression at final concentration of 100 nM using Lipofectamine RNAiMAX (Invitrogen, Thermo Scientific). Simultaneously, specific plasmid (SC111360, Origene) was used to overexpress *CELF4* expression levels at final concentration of 1 μg using Lipofectamine 2000 (Invitrogen, Thermo Scientific). Scrambled siRNA and mock plasmid were used as controls, respectively.

Cell proliferation and drug response assays

Cell proliferation in response to CELF4 modulation and/or drug administrations was evaluated using Alamar-Blue fluorescent assays as previously reported.[15] Briefly, cells were seeded in 96-well plates at a density of 5,000 cells/well, and reduction of Alamar-Blue Reagent (Bio-Source International, Camarillo, CA, USA) was measured at 0, 24, 48, and 72 h with 10% Alamar-Blue after 24 h starvation with 0% fetal bovine serum complete medium by measurement of fluorescent signal exciting at 560 nm and reading at 590 nm (Flex Station 3, Molecular Devices, Sunnyvale, CA, USA). Cells were treated with everolimus (S1120, Selleck Chemicals, Houston, TX, USA), lanreotide (generously provided by IPSEN), and sunitinib (PZ0012, Sigma-Aldrich).

Cell apoptosis assay

After *CELF4* silencing, cells were seeded at a density of 6,000/well in 96-well plates. After 48 h, caspase-3/7 enzymatic activity was measured using Apo-ONE Homogeneous Caspase-3/7 Assay (Promega, Madison, WI, USA) following manufacturer instructions. Briefly, caspase 3/7 substrate was diluted in 1:100 in its commercial buffer and added to the cells. After 3 h incubation, fluorescence was read at 499/521 nm wavelength with the FlexStation 3 Multi-Mode Microplate reader.

RNA isolation, reverse-transcription, and quantitative PCR

Details of RNA quantification, isolation, reverse-transcription, and real-time qPCR have been reported previously.[34] Specific sets of primers for transcripts studied are shown in Table S10. The expression level was adjusted by a normalization factor (NF) obtained from the expression levels of 3 different housekeeping genes (*ACTB*, *GAPDH*, *HPRT1*) using Genorm 3.3.

mTOR phospho-antibody array

To study the potential changes in the mTOR pathway after *CELF4* silencing, we carried out an antibody phosphoarray based on fluorescent detection. Two slides were employed to measure mTOR activity under siCELF4 or scramble (used as control) conditions. All procedures required to perform protein extraction, biotinylation of proteins, its conjugation to antibody array, and detection by Dye-Streptavidin were performed following the manufacturer's instructions with the reagents provided by the assay kit. A total of 5×10^6 QGP-1 and BON-1 cells were seeded in 25 cm^2 flasks, and after 24 h transfection, the culture was washed with 1× PBS 5 times, and cells were collected using a scraper and 200 μL extraction buffer to prevent protein degradation and dephosphorylation. After cell silencing, cells were lysed with a non-denaturing extraction buffer provided in the Antibody Array Assay Kit. Lysate samples protein concentration was measured by UV absorbance A280 using the NanoDrop 2000 (Thermo Scientific). Biotinylation of protein samples was performed with biotin/DMF solution and was detected by Cy3-streptavidin. The conjugation was scanned at the Laboratory of Genetics at Core Research Support Service (University of Cordoba, Cordoba, Spain) using Axon GenePix 4000B. The information regarding specificity, detectability, and reproducibility for the assay can be accessed at the company website.

mTOR phospho-antibody array analysis

Results from the measurement of the mTOR phospho-antibody array were provided by the Laboratory of Genetics at Core Research Support Service (University of Cordoba) as a matrix data array, and its analysis was performed with R packages in our lab. Differential expression between samples with *CELF4* silencing and its scramble was analyzed using an empirical Bayesian method (limma R package).[80] A fold change of <1.5 and a $p < 0.05$ were used to detect phosphosites. Statistical modeling/machine learning techniques provided a way to classify phosphosites and identify relevant underlying biomarkers. In that context, the R package PHONEMeS,[81] which employs boolean logic models of signaling networks downstream of a perturbed kinase to detect signaling mechanisms and drug modes of action, was used. This package needs CPLEX as a network optimiser to improve the output. Molecular signaling classification was profiled by Cytoscape.[82]

Western blot

Cell lines transfected with siRNAs were lysed to analyze protein expression and phosphorylation by western blot, using standard procedures[13] and specific antibodies for phospho-AKT (#4060S, Cell Signaling, Beverly, MA, USA); phospho-TSC2 (BS-3444R, Bioss, Woburn, MA, USA); and TUBB (#2128, Cell Signaling), as well as with the secondary antibody HRP-conjugated goat-anti-rabbit (#7074s; Cell Signaling) immunoglobulin G (IgG). Primary antibodies were used in a 1:1,000 dilution and secondary in 1:2,000. A densitometry

analysis of the bands obtained was carried out with ImageJ software (v.1.5, developed by NIH, Bethesda, MD, USA).

Xenograft model

Two million BON-1 cells were injected in each flank of 7-week-old male athymic BALB/cAnNRj-Foxn1nu mice (Janvier Labs, Le Genest-Saint-Isle, France; n = 5 mice), resuspended in 100 μL basement membrane extract. *CELF4* or scramble (used as control) siRNA was injected into each xenografted tumor by using AteloGene reagent (KOKEN, #KKN1394) to transfect the siRNA molecules into cells by local administrations, according to the manufacturer's instructions, when tumors were measurable. Tumor growth was monitored twice per week for 4 weeks by using a digital caliper, and mice were sacrificed after 15 days of silencing. All experimental procedures were carried out following the European Regulations for Animal Care, in accordance with guidelines and regulations, and under the approval of the University of Córdoba Research Ethics Committee.

Statistical analysis

Samples from all groups were processed at the same time. Statistical differences between two variables were calculated according to normality, assessed by Kolmogorov-Smirnov test, using parametric t test or non-parametric Mann Whitney U test. For groups with three or more variables, one-way ANOVA analysis or Kruskal-Wallis test were performed. To normalize values within treatment and control and minimize intragroup variations in the different experiments, the values obtained were compared with controls (set at 100%). The ROC curves were used to evaluate the suitability of genes to distinguish different groups of samples. Heatmaps were performed through Metaboanalyst software (https://www.metaboanalyst.ca; McGill University, Montreal, QC, Canada). Results from *in vitro* studies were obtained from at least 3 separate independent experiments carried out on different days with different cell preparations. Data were expressed as mean ± SEM, $p < 0.05$ was considered statistically significant, and asterisks indicate significant differences (*$p < 0.05$, **$p < 0.01$, ***$p < 0.001$, ****$p < 0.0001$). Analyses were performed with SPSS v.22 (IBM SPSS Statistics, Chicago, IL, USA) and GraphPad Prism 7 (GraphPad Software, La Jolla, CA, USA).

DATA AND CODE AVAILABILITY

All datasets used and/or analyzed during the current study are available from the corresponding author upon reasonable request. Original raw high-throughput sequencing data have been deposited in Sequence Read Archive (SRA) under accession number SRA: PRJNA1037144.

SUPPLEMENTAL INFORMATION

Supplemental information can be found online at https://doi.org/10.1016/j.omtn.2023.102090.

ACKNOWLEDGMENTS

The authors wish to acknowledge Dr. Mercedes Cousinou and Ms. Laura Redondo at the Department of Genomics, Central Service for Research Support (SCAI), of the University of Cordoba for help with the analysis of the mTOR-phospho-antibody array. We thank all patients and their families for generously donating the samples studies in this work. All techniques carried out in this study were conducted in accordance with the ethical standards of the Helsinki Declaration and of the World Medical Association and with the approval of the University of Cordoba/IMIBIC and ethics committees from all the hospitals involved in the study. Informed consent from each patient was obtained. All experimental procedures with mice were carried out following the European Regulations for Animal Care, in accordance with guidelines and regulations, and under the approval of the University of Cordoba research ethics committees (no. 15-05-2018-088). This work has been supported by the Spanish Ministry of Economy (MINECO; BFU2016–80360-R to J.P.C.) and the Ministry of Science and Innovation (MICINN; PID2019-105201RB-I00 and AEI/10.13039/501100011033 to J.P.C. and PID2019-105564RB-I00 to R.M.L.); Instituto de Salud Carlos III, co-funded by the European Union (ERDF/ESF, "Investing in your future") (FIS grants PI17/02287 and PI20/01301 to M.D.G.; DTS grant DTS20/00050 to R.M.L.; postdoctoral Grant Sara Borrell CD19/00255 to A.I.-C.; and predoctoral contract FI17/00282 to E.A.-P.); the Spanish Ministry of Universities (predoctoral contracts FPU18/02275 to R.B.-E. and FPU20/03958 to V.G.-V. and a postdoctoral contract under the program María Zambrano funded by the European Union Next Generation-EU to S.P.-A.); Junta de Andalucía (BIO-0139); FEDER UCO-202099901918904 (to J.P.C. and A.I.-C.); the Nicolas Monardes Programme from the "Servicio Andaluz de Salud, Junta de Andalucia", Spain C1-0005-2019 (to E.M.Y.-S.); Grupo Español de Tumores Neuroendocrinos y Endocrinos (GETNE2016 and GETNE2019 research grants to J.P.C.); Fundación Eugenio Rodríguez Pascual (FERP2020 grant to J.P.C.); and CIBERobn Fisiopatología de la Obesidad y Nutrición. CIBER is an initiative of Instituto de Salud Carlos III.

AUTHOR CONTRIBUTIONS

Conception of the project, E.A.-P., S.P.-A., A.A.-S., A.I.-C., and J.P.C.; data curation and analysis, E.A.-P., S.P.-A., A.A.-D., R.B.-E., V.G.-V., A.A.-S., R.M.L., A.I.-C., and J.P.C.; methodology, E.A.-P., S.P.-A., A.A.-D., R.B.-E., V.G.-V., E.M.Y.-S., M.E.S.-F., R.S.-B., M.A.G.-M., F.G.-N., M.D.G., A.A.-S., R.M.L., A.I.-C., and J.P.C.; writing, E.A.-P., S.P.-A., F.G.-N., M.D.G., R.M.L., A.I.-C., and J.P.C.; review and editing, E.A.-P., S.P.-A., A.A.-D., R.B.-E., V.G.-V., E.M.Y.-S., M.E.S.-F., R.S.-B., M.A.G.-M., F.G.-N., M.D.G., A.A.-S., R.M.L., A.I.-C., and J.P.C.; resources, M.E.S.-F., R.S.-B., M.A.G.-M., F.G.-N., M.D.G., A.A.-S., R.M.L., A.I.-C., and J.P.C.; supervision, S.P.-A., R.M.L., A.I.-C., and J.P.C.; funding: R.M.L., A.I.-C., and J.P.C.

DECLARATION OF INTERESTS

The authors declare no competing interests.

REFERENCES

1. Pedraza-Arévalo, S., Gahete, M.D., Alors-Pérez, E., Luque, R.M., and Castaño, J.P. (2018). Multilayered heterogeneity as an intrinsic hallmark of neuroendocrine tumors. Rev. Endocr. Metab. Disord. *19*, 179–192.

2. Sonbol, M.B., Mazza, G.L., Mi, L., Oliver, T., Starr, J., Gudmundsdottir, H., Cleary, S.P., Hobday, T., and Halfdanarson, T.R. (2022). Survival and Incidence Patterns

of Pancreatic Neuroendocrine Tumors Over the Last 2 Decades: A SEER Database Analysis. Oncol. *27*, 573–578.

3. Darbà, J., and Marsà, A. (2019). Exploring the current status of neuroendocrine tumours: a population-based analysis of epidemiology, management and use of resources. BMC Cancer *19*, 1226.
4. Raphael, M.J., Chan, D.L., Law, C., and Singh, S. (2017). Principles of diagnosis and management of neuroendocrine tumours. CMAJ (Can. Med. Assoc. J.) *189*, E398–E404.
5. Leyden, S., Kolarova, T., Bouvier, C., Caplin, M., Conroy, S., Davies, P., Dureja, S., Falconi, M., Ferolla, P., Fisher, G., et al. (2020). Unmet needs in the international neuroendocrine tumor (NET) community: Assessment of major gaps from the perspective of patients, patient advocates and NET health care professionals. Int. J. Cancer *146*, 1316–1323.
6. Mafficini, A., and Scarpa, A. (2018). Genomic landscape of pancreatic neuroendocrine tumours: the International Cancer Genome Consortium. J. Endocrinol. *236*, R161–R167.
7. Mafficini, A., and Scarpa, A. (2019). Genetics and Epigenetics of Gastroenteropancreatic Neuroendocrine Neoplasms. Endocr. Rev. *40*, 506–536.
8. Lee, S.C.W., and Abdel-Wahab, O. (2016). Therapeutic targeting of splicing in cancer. Nat. Med. *22*, 976–986.
9. Hanahan, D., and Weinberg, R.A. (2011). Hallmarks of cancer: the next generation. Cell *144*, 646–674.
10. Bonnal, S.C., López-Oreja, I., and Valcárcel, J. (2020). Roles and mechanisms of alternative splicing in cancer - implications for care. Nat. Rev. Clin. Oncol. *17*, 457–474.
11. Sampedro-Núñez, M., Luque, R.M., Ramos-Levi, A.M., Gahete, M.D., Serrano-Somavilla, A., Villa-Osaba, A., Adrados, M., Ibáñez-Costa, A., Martín-Pérez, E., Culler, M.D., et al. (2016). Presence of sst5TMD4, a truncated splice variant of the somatostatin receptor subtype 5, is associated to features of increased aggressiveness in pancreatic neuroendocrine tumors. Oncotarget *7*, 6593–6608.
12. Luque, R.M., Sampedro-Nuñez, M., Gahete, M.D., Ramos-Levi, A., Ibáñez-Costa, A., Rivero-Cortés, E., Serrano-Somavilla, A., Adrados, M., Culler, M.D., Castaño, J.P., and Marazuela, M. (2015). In1-ghrelin, a splice variant of ghrelin gene, is associated with the evolution and aggressiveness of human neuroendocrine tumors: Evidence from clinical, cellular and molecular parameters. Oncotarget *6*, 19619–19633.
13. Durán-Prado, M., Gahete, M.D., Hergueta-Redondo, M., Martínez-Fuentes, A.J., Córdoba-Chacón, J., Palacios, J., Gracia-Navarro, F., Moreno-Bueno, G., Malagón, M.M., Luque, R.M., and Castaño, J.P. (2012). The new truncated somatostatin receptor variant sst5TMD4 is associated to poor prognosis in breast cancer and increases malignancy in MCF-7 cells. Oncogene *31*, 2049–2061.
14. Durán-Prado, M., Saveanu, A., Luque, R.M., Gahete, M.D., Gracia-Navarro, F., Jaquet, P., Dufour, H., Malagón, M.M., Culler, M.D., Barlier, A., and Castaño, J.P. (2010). A potential inhibitory role for the new truncated variant of somatostatin receptor 5, sst5TMD4, in pituitary adenomas poorly responsive to somatostatin analogs. J. Clin. Endocrinol. Metab. *95*, 2497–2502.
15. Hormaechea-Agulla, D., Jiménez-Vacas, J.M., Gómez-Gómez, E., L-López, F., Carrasco-Valiente, J., Valero-Rosa, J., Moreno, M.M., Sánchez-Sánchez, R., Ortega-Salas, R., Gracia-Navarro, F., et al. (2017). The oncogenic role of the spliced somatostatin receptor sst5TMD4 variant in prostate cancer. Faseb. J. *31*, 4682–4696.
16. Puig-Domingo, M., Luque, R.M., Reverter, J.L., López-Sánchez, L.M., Gahete, M.D., Culler, M.D., Díaz-Soto, G., Lomeña, F., Squarcia, M., Mate, J.L., et al. (2014). The truncated isoform of somatostatin receptor5 (sst5TMD4) is associated with poorly differentiated thyroid cancer. PLoS One *9*, e85527.
17. Rincón-Fernández, D., Culler, M.D., Tsomaia, N., Moreno-Bueno, G., Luque, R.M., Gahete, M.D., and Castaño, J.P. (2018). In1-ghrelin splicing variant is associated with reduced disease-free survival of breast cancer patients and increases malignancy of breast cancer cells lines. Carcinogenesis *39*, 447–457.
18. Hormaechea-Agulla, D., Gahete, M.D., Jiménez-Vacas, J.M., Gómez-Gómez, E., Ibáñez-Costa, A., L-López, F., Rivero-Cortés, E., Sarmento-Cabral, A., Valero-Rosa, J., Carrasco-Valiente, J., et al. (2017). The oncogenic role of the In1-ghrelin splicing variant in prostate cancer aggressiveness. Mol. Cancer *16*, 146.
19. Ibáñez-Costa, A., Gahete, M.D., Rivero-Cortés, E., Rincón-Fernández, D., Nelson, R., Beltrán, M., de la Riva, A., Japón, M.A., Venegas-Moreno, E., Gálvez, M.Á., et al. (2015). In1-ghrelin splicing variant is overexpressed in pituitary adenomas and increases their aggressive features. Sci. Rep. *5*, 8714.
20. Pedraza-Arevalo, S., Alors-Pérez, E., Blázquez-Encinas, R., Herrera-Martinez, A.D., Jiménez-Vacas, J.M., Fuentes-Fayos, A.C., Reyes, O., Ventura, S., Sánchez-Sánchez, R., Ortega-Salas, R., et al. (2022). Spliceosomic dysregulation unveils NOVA1 as a candidate actionable therapeutic target in pancreatic neuroendocrine tumors. Transl. Res.
21. Nasiri-Aghdam, M., Garcia-Garduño, T.C., and Jave-Suárez, L.F. (2021). CELF Family Proteins in Cancer: Highlights on the RNA-Binding Protein/Noncoding RNA Regulatory Axis. Int. J. Mol. Sci. *22*, 11056.
22. Dasgupta, T., and Ladd, A.N. (2012). The importance of CELF control: molecular and biological roles of the CUG-BP, Elav-like family of RNA-binding proteins. Wiley Interdiscip. Rev. RNA *3*, 104–121.
23. Wagnon, J.L., Briese, M., Sun, W., Mahaffey, C.L., Curk, T., Rot, G., Ule, J., and Frankel, W.N. (2012). CELF4 regulates translation and local abundance of a vast set of mRNAs, including genes associated with regulation of synaptic function. PLoS Genet. *8*, e1003067.
24. Yang, Y., Mahaffey, C.L., Bérubé, N., Maddatu, T.P., Cox, G.A., and Frankel, W.N. (2007). Complex seizure disorder caused by Brunol4 deficiency in mice. PLoS Genet. *3*, e124.
25. Sun, W., Wagnon, J.L., Mahaffey, C.L., Briese, M., Ule, J., and Frankel, W.N. (2013). Aberrant sodium channel activity in the complex seizure disorder of Celf4 mutant mice. J. Physiol. *591*, 241–255.
26. Karunakaran, D.K.P., Congdon, S., Guerrette, T., Banday, A.R., Lemoine, C., Chhaya, N., and Kanadia, R. (2013). The expression analysis of Sfrs10 and Celf4 during mouse retinal development. Gene Expr. Patterns *13*, 425–436.
27. Chang, K., Yuan, C., and Liu, X. (2021). A New RBPs-Related Signature Predicts the Prognosis of Colon Adenocarcinoma Patients. Front. Oncol. *11*, 627504.
28. Teerlink, C.C., Stevens, J., Hernandez, R., Facelli, J.C., and Cannon-Albright, L.A. (2021). An intronic variant in the CELF4 gene is associated with risk for colorectal cancer. Cancer Epidemiol. *72*, 101941.
29. Huang, R.L., Su, P.H., Liao, Y.P., Wu, T.I., Hsu, Y.T., Lin, W.Y., Wang, H.C., Weng, Y.C., Ou, Y.C., Huang, T.H.M., and Lai, H.C. (2017). Integrated Epigenomics Analysis Reveals a DNA Methylation Panel for Endometrial Cancer Detection Using Cervical Scrapings. Clin. Cancer Res. *23*, 263–272.
30. Climente-González, H., Porta-Pardo, E., Godzik, A., and Eyras, E. (2017). The Functional Impact of Alternative Splicing in Cancer. Cell Rep. *20*, 2215–2226.
31. Coltri, P.P., Dos Santos, M.G.P., and da Silva, G.H.G. (2019). Splicing and cancer: Challenges and opportunities. Wiley Interdiscip. Rev. RNA *10*, e1527.
32. Gil-Bernabé, A.M., Lucotti, S., and Muschel, R.J. (2013). Coagulation and metastasis: what does the experimental literature tell us? Br. J. Haematol. *162*, 433–441.
33. Siddaway, R., Milos, S., Vadivel, A.K.A., Dobson, T.H.W., Swaminathan, J., Ryall, S., Pajovic, S., Patel, P.G., Nazarian, J., Becher, O., et al. (2022). Splicing is an alternate oncogenic pathway activation mechanism in glioma. Nat. Commun. *13*, 588.
34. Alors-Perez, E., Blázquez-Encinas, R., Alcalá, S., Viyuela-García, C., Pedraza-Arevalo, S., Herrero-Aguayo, V., Jiménez-Vacas, J.M., Mafficini, A., Sánchez-Frías, M.E., Cano, M.T., et al. (2021). Dysregulated splicing factor SF3B1 unveils a dual therapeutic vulnerability to target pancreatic cancer cells and cancer stem cells with an anti-splicing drug. J. Exp. Clin. Cancer Res. *40*, 382.
35. Jiménez-Vacas, J.M., Herrero-Aguayo, V., Gómez-Gómez, E., León-González, A.J., Sáez-Martínez, P., Alors-Pérez, E., Fuentes-Fayos, A.C., Martínez-López, A., Sánchez-Sánchez, R., González-Serrano, T., et al. (2019). Spliceosome component SF3B1 as novel prognostic biomarker and therapeutic target for prostate cancer. Transl. Res. *212*, 89–103.
36. López-Cánovas, J.L., Del Río-Moreno, M., García-Fernandez, H., Jiménez-Vacas, J.M., Moreno-Montilla, M.T., Sánchez-Frias, M.E., Amado, V., L-López, F., Fondevila, M.F., Ciria, R., et al. (2021). Splicing factor SF3B1 is overexpressed and implicated in the aggressiveness and survival of hepatocellular carcinoma. Cancer Lett. *496*, 72–83.
37. Fuentes-Fayos, A.C., Pérez-Gómez, J.M., G-García, M.E., Jiménez-Vacas, J.M., Blanco-Acevedo, C., Sánchez-Sánchez, R., Solivera, J., Breunig, J.J., Gahete, M.D., Castaño, J.P., and Luque, R.M. (2022). SF3B1 inhibition disrupts malignancy and

prolongs survival in glioblastoma patients through BCL2L1 splicing and mTOR/ss-catenin pathways imbalances. J. Exp. Clin. Cancer Res. *41*, 39.

38. Briest, F., and Grabowski, P. (2015). The p53 network as therapeutic target in gastroenteropancreatic neuroendocrine neoplasms. Cancer Treat Rev. *41*, 423–430.

39. Lubomierski, N., Kersting, M., Bert, T., Muench, K., Wulbrand, U., Schuermann, M., Bartsch, D., and Simon, B. (2001). Tumor suppressor genes in the 9p21 gene cluster are selective targets of inactivation in neuroendocrine gastroenteropancreatic tumors. Cancer Res. *61*, 5905–5910.

40. van Riet, J., van de Werken, H.J.G., Cuppen, E., Eskens, F.A.L.M., Tesselaar, M., van Veenendaal, L.M., Klümpen, H.J., Dercksen, M.W., Valk, G.D., Lolkema, M.P., et al. (2021). The genomic landscape of 85 advanced neuroendocrine neoplasms reveals subtype-heterogeneity and potential therapeutic targets. Nat. Commun. *12*, 4612.

41. Scarpa, A., Chang, D.K., Nones, K., Corbo, V., Patch, A.M., Bailey, P., Lawlor, R.T., Johns, A.L., Miller, D.K., Mafficini, A., et al. (2017). Whole-genome landscape of pancreatic neuroendocrine tumours. Nature *543*, 65–71.

42. Vázquez-Borrego, M.C., Fuentes-Fayos, A.C., Venegas-Moreno, E., Rivero-Cortés, E., Dios, E., Moreno-Moreno, P., Madrazo-Atutxa, A., Remón, P., Solivera, J., Wildemberg, L.E., et al. (2019). Splicing machinery is dysregulated in pituitary neuroendocrine tumors and is associated with aggressiveness features. Cancers *11*, 1439.

43. Wang, H., Zhang, C.Z., Lu, S.X., Zhang, M.F., Liu, L.L., Luo, R.Z., Yang, X., Wang, C.H., Chen, S.L., He, Y.F., et al. (2019). A Coiled-Coil Domain Containing 50 Splice Variant Is Modulated by Serine/Arginine-Rich Splicing Factor 3 and Promotes Hepatocellular Carcinoma in Mice by the Ras Signaling Pathway. Hepatology *69*, 179–195.

44. Yao, J.C., Shah, M.H., Ito, T., Bohas, C.L., Wolin, E.M., Van Cutsem, E., Hobday, T.J., Okusaka, T., Capdevila, J., de Vries, E.G.E., et al. (2011). Everolimus for advanced pancreatic neuroendocrine tumors. N. Engl. J. Med. *364*, 514–523.

45. Hofving, T., Arvidsson, Y., Almobarak, B., Inge, L., Pfragner, R., Persson, M., Stenman, G., Kristiansson, E., Johanson, V., and Nilsson, O. (2018). The neuroendocrine phenotype, genomic profile and therapeutic sensitivity of GEPNET cell lines. Endocr. Relat. Cancer *25*, X1–X2.

46. Vandamme, T., Peeters, M., Dogan, F., Pauwels, P., Van Assche, E., Beyens, M., Mortier, G., Vandeweyer, G., de Herder, W., Van Camp, G., et al. (2015). Whole-exome characterization of pancreatic neuroendocrine tumor cell lines BON-1 and QGP-1. J. Mol. Endocrinol. *54*, 137–147.

47. Khanna, L., Prasad, S.R., Sunnapwar, A., Kondapaneni, S., Dasyam, A., Tammisetti, V.S., Salman, U., Nazarullah, A., and Katabathina, V.S. (2020). Pancreatic Neuroendocrine Neoplasms: 2020 Update on Pathologic and Imaging Findings and Classification. Radiographics *40*, 1240–1262.

48. Taskin, O.C., Clarke, C.N., Erkan, M., Tsai, S., Evans, D.B., and Adsay, V. (2020). Pancreatic neuroendocrine neoplasms: current state and ongoing controversies on terminology, classification and prognostication. J. Gastrointest. Oncol. *11*, 548–558.

49. Lakis, V., Lawlor, R.T., Newell, F., Patch, A.M., Mafficini, A., Sadanandam, A., Koufariotis, L.T., Johnston, R.L., Leonard, C., Wood, S., et al. (2021). DNA methylation patterns identify subgroups of pancreatic neuroendocrine tumors with clinical association. Commun. Biol. *4*, 155.

50. Luo, L., Sun, W., Zhu, W., Li, S., Zhang, W., Xu, X., Fang, D., Grahn, T.H.M., Jiang, L., and Zheng, Y. (2021). BCAT1 decreases the sensitivity of cancer cells to cisplatin by regulating mTOR-mediated autophagy via branched-chain amino acid metabolism. Cell Death Dis. *12*, 169.

51. Liu, J.C., Granieri, L., Shrestha, M., Wang, D.Y., Vorobieva, I., Rubie, E.A., Jones, R., Ju, Y., Pellecchia, G., Jiang, Z., et al. (2018). Identification of CDC25 as a Common Therapeutic Target for Triple-Negative Breast Cancer. Cell Rep. *23*, 112–126.

52. Geng, Q., Liu, J., Gong, Z., Chen, S., Chen, S., Li, X., Lu, Y., Zhu, X., Lin, H.K., and Xu, D. (2017). Phosphorylation by mTORC1 stablizes Skp2 and regulates its oncogenic function in gastric cancer. Mol. Cancer *16*, 83.

53. He, C.L., Bian, Y.Y., Xue, Y., Liu, Z.X., Zhou, K.Q., Yao, C.F., Lin, Y., Zou, H.F., Luo, F.X., Qu, Y.Y., et al. (2016). Pyruvate Kinase M2 Activates mTORC1 by Phosphorylating AKT1S1. Sci. Rep. *6*, 21524.

54. Ben-Sahra, I., Hoxhaj, G., Ricoult, S.J.H., Asara, J.M., and Manning, B.D. (2016). mTORC1 induces purine synthesis through control of the mitochondrial tetrahydrofolate cycle. Science *351*, 728–733.

55. Sugiura, A., Andrejeva, G., Voss, K., Heintzman, D.R., Xu, X., Madden, M.Z., Ye, X., Beier, K.L., Chowdhury, N.U., Wolf, M.M., et al. (2022). MTHFD2 is a metabolic checkpoint controlling effector and regulatory T cell fate and function. Immunity *55*, 65–81.e9.

56. He, Z., Hu, X., Liu, W., Dorrance, A., Garzon, R., Houghton, P.J., and Shen, C. (2017). P53 suppresses ribonucleotide reductase via inhibiting mTORC1. Oncotarget *8*, 41422–41431.

57. Shan, J., Wang, Z., Mo, Q., Long, J., Fan, Y., Cheng, L., Zhang, T., Liu, X., and Wang, X. (2022). Ribonucleotide reductase M2 subunit silencing suppresses tumorigenesis in pancreatic cancer via inactivation of PI3K/AKT/mTOR pathway. Pancreatology *22*, 401–413.

58. White, M.A., Lin, C., Rajapakshe, K., Dong, J., Shi, Y., Tsouko, E., Mukhopadhyay, R., Jasso, D., Dawood, W., Coarfa, C., and Frigo, D.E. (2017). Glutamine Transporters Are Targets of Multiple Oncogenic Signaling Pathways in Prostate Cancer. Mol. Cancer Res. *15*, 1017–1028.

59. Li, F., Hu, G., Long, X., Cao, Y., Li, Q., Guo, W., Wang, J., Liu, J., and Fu, S. (2022). Stearic Acid Activates the PI3K-mTOR-4EBP1/S6K and mTOR-SREBP-1 Signaling Axes through FATP4-CDK1 To Promote Milk Synthesis in Primary Bovine Mammary Epithelial Cells. J. Agric. Food Chem. *70*, 4007–4018.

60. Sheng, J., Zhao, Q., Zhao, J., Zhang, W., Sun, Y., Qin, P., Lv, Y., Bai, L., Yang, Q., Chen, L., et al. (2018). SRSF1 modulates PTPMT1 alternative splicing to regulate lung cancer cell radioresistance. EBioMedicine *38*, 113–126.

61. Liu, G.Y., and Sabatini, D.M. (2020). Author Correction: mTOR at the nexus of nutrition, growth, ageing and disease. Nat. Rev. Mol. Cell Biol. *21*, 246.

62. Saxton, R.A., and Sabatini, D.M. (2017). mTOR Signaling in Growth, Metabolism, and Disease. Cell *168*, 960–976.

63. Missiaglia, E., Dalai, I., Barbi, S., Beghelli, S., Falconi, M., della Peruta, M., Piemonti, L., Capurso, G., Di Florio, A., delle Fave, G., et al. (2010). Pancreatic endocrine tumors: expression profiling evidences a role for AKT-mTOR pathway. J. Clin. Oncol. *28*, 245–255.

64. Zanini, S., Renzi, S., Giovinazzo, F., and Bermano, G. (2020). mTOR Pathway in Gastroenteropancreatic Neuroendocrine Tumor (GEP-NETs). Front. Endocrinol. *11*, 562505.

65. Chan, J., and Kulke, M. (2014). Targeting the mTOR signaling pathway in neuroendocrine tumors. Curr. Treat. Options Oncol. *15*, 365–379.

66. Downward, J. (1999). How BAD phosphorylation is good for survival. Nat. Cell Biol. *1*, E33–E35.

67. Lin, A., Yao, J., Zhuang, L., Wang, D., Han, J., Lam, E.W.F., and Gan, B. (2014). The FoxO-BNIP3 axis exerts a unique regulation of mTORC1 and cell survival under energy stress. Oncogene *33*, 3183–3194.

68. Zhang, Y., Shen, K., Bai, Y., Lv, X., Huang, R., Zhang, W., Chao, J., Nguyen, L.K., Hua, J., Gan, G., et al. (2016). Mir143-BBC3 cascade reduces microglial survival via interplay between apoptosis and autophagy: Implications for methamphetamine-mediated neurotoxicity. Autophagy *12*, 1538–1559.

69. Warren, C.F.A., Wong-Brown, M.W., and Bowden, N.A. (2019). BCL-2 family isoforms in apoptosis and cancer. Cell Death Dis. *10*, 177.

70. Chan, C.S., Laddha, S.V., Lewis, P.W., Koletsky, M.S., Robzyk, K., Da Silva, E., Torres, P.J., Untch, B.R., Li, J., Bose, P., et al. (2018). ATRX, DAXX or MEN1 mutant pancreatic neuroendocrine tumors are a distinct alpha-cell signature subgroup. Nat. Commun. *9*, 4158.

71. Kim, D., Pertea, G., Trapnell, C., Pimentel, H., Kelley, R., and Salzberg, S.L. (2013). TopHat2: accurate alignment of transcriptomes in the presence of insertions, deletions and gene fusions. Genome Biol. *14*, R36.

72. Anders, S., Pyl, P.T., and Huber, W. (2015). HTSeq–a Python framework to work with high-throughput sequencing data. Bioinformatics *31*, 166–169.

73. Anders, S., and Huber, W. (2010). Differential expression analysis for sequence count data. Genome Biol. *11*, R106.

74. Scrucca, L., Fop, M., Murphy, T.B., and Raftery, A.E. (2016). mclust 5: Clustering, Classification and Density Estimation Using Gaussian Finite Mixture Models. Rom. Jahrb. *8*, 289–317.

75. Subramanian, A., Tamayo, P., Mootha, V.K., Mukherjee, S., Ebert, B.L., Gillette, M.A., Paulovich, A., Pomeroy, S.L., Golub, T.R., Lander, E.S., and Mesirov, J.P. (2005). Gene

set enrichment analysis: a knowledge-based approach for interpreting genome-wide expression profiles. Proc. Natl. Acad. Sci. USA *102*, 15545–15550.

76. Huang, D.W., Sherman, B.T., and Lempicki, R.A. (2009). Bioinformatics enrichment tools: paths toward the comprehensive functional analysis of large gene lists. Nucleic Acids Res. *37*, 1–13.

77. Patro, R., Duggal, G., Love, M.I., Irizarry, R.A., and Kingsford, C. (2017). Salmon provides fast and bias-aware quantification of transcript expression. Nat. Methods *14*, 417–419.

78. Frankish, A., Diekhans, M., Ferreira, A.M., Johnson, R., Jungreis, I., Loveland, J., Mudge, J.M., Sisu, C., Wright, J., Armstrong, J., et al. (2019). GENCODE reference annotation for the human and mouse genomes. Nucleic Acids Res. *47*, D766–D773.

79. Trincado, J.L., Entizne, J.C., Hysenaj, G., Singh, B., Skalic, M., Elliott, D.J., and Eyras, E. (2018). SUPPA2: fast, accurate, and uncertainty-aware differential splicing analysis across multiple conditions. Genome Biol. *19*, 40.

80. Smyth, G.K. (2004). Linear models and empirical bayes methods for assessing differential expression in microarray experiments. Stat. Appl. Genet. Mol. Biol. *3*. Article3.

81. Terfve, C.D.A., Wilkes, E.H., Casado, P., Cutillas, P.R., and Saez-Rodriguez, J. (2015). Large-scale models of signal propagation in human cells derived from discovery phosphoproteomic data. Nat. Commun. *6*, 8033.

82. Shannon, P., Markiel, A., Ozier, O., Baliga, N.S., Wang, J.T., Ramage, D., Amin, N., Schwikowski, B., and Ideker, T. (2003). Cytoscape: a software environment for integrated models of biomolecular interaction networks. Genome Res. *13*, 2498–2504.